10.18462/iir.gl.2018.1206

THE R744 MULTI-EJECTOR HYBRID CFD AND EXPERIMENTALLY-BASED REDUCED-ORDER MODEL

Michal Haida[(a)], Jacek Smolka[(a)], Armin Hafner[(b)], Michal Palacz[(a)], Ziemowit Ostrowski[(a)], Kenneth B. Madsen[(c)], Sven Försterling[(d)], Andrzej J. Nowak[(a)], Krzysztof Banasiak[(e)]

[(a)] Institute of Thermal Technology, Silesian University of Technology
Gliwice, 44-100, Poland, Michal.Haida@polsl.pl
[(b)] NTNU, Trondheim, 7465, Norway, Armin.Hafner@ntnu.no
[(c)] Danfoss A/S, Nordborg, 6430, Denmark, kbm@danfoss.com
[(d)]TLK-Thermo GmbH, Braunschweig, 38106, Germany, s.foersterling@tlk-thermo.de
[(e)] SINTEF Energy Research, Trondheim, 7465, Norway, Krzysztof.Banasiak@sintef.no

ABSTRACT

The proposed hybrid reduced-order model (HROM) of the four R744 fixed ejectors installed in the multi-ejector module is presented. The ejectors HROM was built by use of the proper orthogonal decomposition together with the radial basis function interpolation to obtain high-accuracy model for a wide range of the subcritical and transcritical operating regimes. The input data for the proposed model was the combination of the experimental data of the investigated ejectors together with the numerical results obtained by use of the *ejectorPL* platform. The proposed HROM of each R744 vapour fixed ejector obtained a satisfactory accuracy of the motive and the suction nozzle mass flow rates for most validated points and significantly reduced the computational time. Hence, the proposed HROM of the R744 vapour fixed ejectors was successfully implemented to the Modelica dynamic simulations of the R744 refrigeration system to evaluate the system energy performance corresponding to the real ejector performance at different operating conditions.

Keywords: R744, refrigeration application, two-phase ejector, numerical model, reduced-order model

1. INTRODUCTION

Due to the restrictive legal regulations for environmental protection in refrigeration, common synthetic refrigerants are replaced by environmentally friendly natural refrigerants, such as carbon dioxide denoted as R744 (United Nations Environment and Ozone, 1987). The satisfactory thermal properties of CO_2 as well as its non-flammability, non-toxicity and the availability in the market let to utilise R744 in the supermarket refrigeration applications (Kim et al., 2004). The energy performance analysis of the R744 refrigeration system indicated the necessity to improve the system coefficient of performance (COP) in warm climates due to high thermodynamic losses during operation of the system in the transcritical mode. Therefore, the several modifications were done to improve the system energy performance i.e. the R744 transcritical booster system with the parallel compression (Sharma et al., 2014).

The energy performance improvement of the R744 booster system with the parallel compression can be done by use of the ejector as the main expansion device to recover some potentially work (Elbel and Hrnjak, 2004). The COP improvement of the R744 ejector-based refrigeration system was indicated in the literature (Besagni et al., 2016). The CO_2 supermarket refrigeration system operates at a different ambient temperature and different cooling demand, which were varied during the daytime. Therefore, the several different fixed-geometry ejectors that can be operated in single mode or parallel mode were investigated. The multi-ejector concept was presented by Hafner et al. (2014), which investigate the energy performance of the R744 multi-ejector supermarket refrigeration system for different European climate zones. The authors showed the satisfactory system energy performance improvement up to 30 % when compared to the reference CO_2 booster system with flash gas bypass. Moreover, Hafner et al. (2014) stated that the system control strategy of the multi-ejector system for supermarket application should be optimised to further improve the system efficiency in different climate zones.

The R744 multi-ejector expansion pack was designed, manufactured and investigated in the work of Banasiak et al. (2015). The developed module was equipped with the four different ejector cartridges to enable a discrete opening characteristic with a binary profile for the R744 vapour compression system. The experimental campaign was carried out to map the performance of individual ejectors at the operating conditions typical for refrigeration system in the supermarket. Moreover, the authors proposed the functions for the smallest ejector to calculate the motive nozzle mass flow rate (MFR) and the ratio between suction nozzle MFR and motive nozzle MFR called the mass entrainment ratio.

Integration of the heating, ventilation and air-conditioning systems with the refrigeration system (HVAC&R) in a supermarket application reduced the total electric power consumption of the system by more than 15% (Cecchinato et al., 2010). The theoretical analysis of the CO_2 multi-ejector refrigeration and air-conditioning system was done by Gullo et al. (2017). The investigated system with the multi-ejector developed by Banasiak et al. (2015) was compared with the R404A direct expansion system and various configuration of the R744 booster refrigeration system with and without the parallel compression. The authors stated that the energy savings of the multi-ejector system were in the range from 15 % to 27 % when compared to the R404A direct expansion system.

The theoretical investigations of the R744 multi-ejector HVAC&R supermarket system were done based on the empirical functions of the multi-ejector module provided by experimental results at specified operating conditions, thereby the proposed functions can be used only within the specified operating points. The performance of the ejector can also be calculated based on the non-dimensional model (Kornhauser, 1990). However, the foregoing model assumed the efficiency of the ejector, which resulted on the low accuracy at wide range in the supermarket application. The calculations of the ejector at high accuracy for refrigeration and air-conditioning operating conditions can be done by use of the reduced-order model (ROM) based on the proper orthogonal decomposition basis with radial basis function (trained POD-RBF). The POD-RBF approach was used for R744 two-phase ejector by Haida et al. (2018a). The proposed model was generated based on the training data being CFD results of the CO_2 ejector HEM model for the operating conditions close to the critical point. The authors stated that the numerical and experimental validation of the POD-RBF ejector model confirmed high accuracy of ROM within ±10% for most of the investigated points. This approach let to combine the experimental data and the results of the numerical CFD model of the single ejector to generate the ROM basis for fast computation of the single operational point. Moreover, ROM allows the functional computation of the R744 ejector within the selected operating points.

The main aim of this paper is to present the performance mapping of the fixed ejectors installed in multi-ejector modules integrated with the CO_2 HVAC&R supermarket refrigeration system. The hybrid reduced-order model (HROM) of each ejector was developed based on the experimental data given from the experimental test facility at SINTEF Energy Research laboratory in Trondheim and the results from the enhanced CFD model of the two-phase ejector performed by use of the *ejectorPL* platform (Haida et al., 2018b). The fast computations of the HROM let to use the proposed model in the dynamic simulations. The performance mapping was done to present the mass entrainment ratio of the investigated ejectors at a wide range of the operating conditions. Moreover, the investigation of the pressure lift on the ejectors performance at the operating conditions typical for the supermarket refrigeration system was presented in this paper. The proposed HROM is being implemented in *TIL model library* to perform the Dynamic simulation of the R744 multi-ejector supermarket system at a wide operating conditions.

2. THE R744 MULTI-EJECTOR MODULE

The recent R744 supermarket HVAC&R systems were equipped with the multi-ejector module to cover the varied cooling demand in the R744 supermarket refrigeration system. Figure 1 presents the layout of the R744 multi-ejector module with the inlets and outlet collectors. The module contained four fixed ejectors with different sizes. Thus, the capacity of each individual ejector increased in binary order (1:2:4:8). The solenoid valves installed in the motive collector let to utilise the ejectors in single or parallel operation. The motive stream entered from the gas cooler outlet and the suction flow was entrained from the medium-temperature (MT) liquid receiver outside the MT evaporator. The outlet mixed stream flowed to the intermediate-pressure liquid receiver directly connected with the air-conditioning (AC) evaporator. Therefore, the outlet conditions of the multi-ejector were defined based on the AC operational mode. The fixed ejectors were designed and manufactured in cooperation of SINTEF-SUT-DANFOSS based on the CFD model developed in the work of Smolka et al. (2013). Moreover, the multi-ejector model was manufactured and the performance mapping of each ejector was done for the refrigeration system operating conditions by Banasiak et al. (2015). The main dimensions of each fixed ejector were set in Table 1.

10.18462/iir.gl.2018.1206

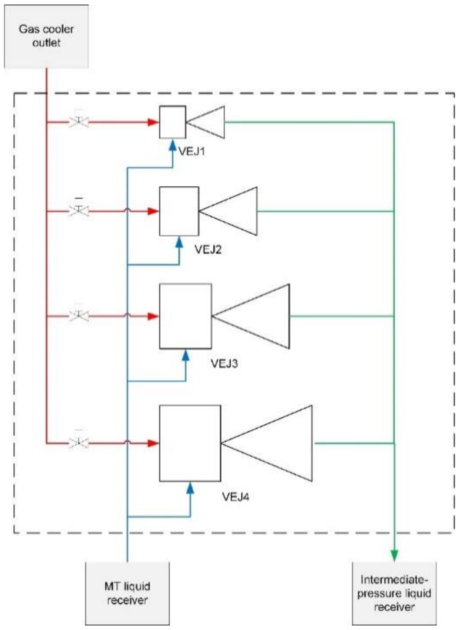

Figure 1. The R744 multi-ejector module.

Table 1. The main geometry parameters of the fixed ejectors installed in the R744 multi-ejector module (Banasiak et al., 2015).

Parameters name	Unit	VEJ1	VEJ2	VEJ3	VEJ4
Motive nozzle inlet diameter	mm	3.80	3.80	3.80	3.80
Motive nozzle throat diameter	mm	1.00	1.41	2.00	2.83
Motive nozzle outlet diameter	mm	1.12	1.58	2.24	3.16
Motive nozzle converging angle	°	30.00	30.00	30.00	30.00
Motive nozzle diverging angle	°	2.00	2.00	2.00	2.00
Diffuser outlet diameter	mm	7.30	8.40	10.30	13.10
Diffuser angle	°	5.00	5.00	5.00	5.00

The performance mapping of the fixed ejectors installed in the multi-ejector module was performed at much wider operating regime when compared to Banasiak et al. (2015) to investigate the ejector efficiency of the ejector in the CO_2 HVAC&R supermarket system. The operational envelope for the motive nozzle and the suction nozzle of the ejectors was presented in Figure 2. It can be seen that the motive nozzle pressure in Figure 2(a) was defined in the range from 50 bar to 140 bar to analyse the ejector performance in subcritical and transcritical operating mode at various ambient temperature. In addition, the different subcooling of the gas cooler was investigated. The suction nozzle operating conditions presented in Figure 2(b) were defined to analyse the ejector mapping performance for superheated vapour with the superheat below 15 °C, saturated vapour and two-phase flow with quality above 0.8. Moreover, the suction nozzle pressure varied in the range from 26 bar to 46 bar related to the refrigeration, AC and heat pump conditions. The outlet conditions were defined by the definition of the pressure lift Δp, which is a difference between the outlet pressure and the suction nozzle pressure. In the presented investigation, the pressure lift for all ejectors was in the range from 4 bar to 15 bar.

The wide operating range required the use of a complex mathematical model to predict the two nozzles' MFRs for each ejector. However, the mathematical model should be adapted to perform the ejector calculation in the dynamic simulation of the CO_2 HVAC&R supermarket system in the energy performance analysis of the system. Therefore, the proposed HROM was used in the presented investigation as the main benefits of ROM is fast computations and high accuracy of the mass flow rates prediction.

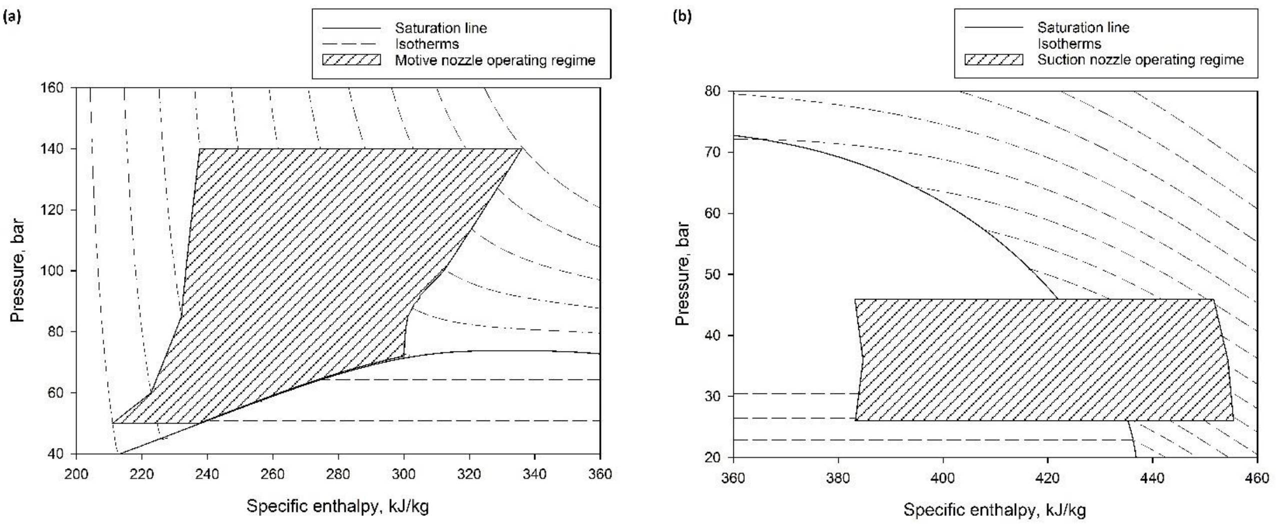

Figure 2. The R744 HROM multi-ejector operating regime: (a) motive nozzle; (b) suction nozzle.

3. HYBRID REDUCED-ORDER MODEL

3.1 The POD-RBF approach

The POD approach to constructing the optimal approximation based on the set of *N* sampled values of the two-phase flow parameters inside the ejector stored in a single vector called the snapshot (Ostrowski et al., 2008). Thus, the snapshot rectangular matrix **U** is generated for *M* snapshot vectors related to the number of the considered operating points (being the input parameters used to generate the snapshots). Snapshot vectors related to the number of the input parameters. The aim of the POD model is to define the orthogonal matrix **Φ** by reconstructing the basis snapshot matrix **U** based on the linear combination of the snapshots:

$$\mathbf{\Phi} = \mathbf{U} \cdot \mathbf{V} \qquad (1)$$

where **V** is the modal matrix. The POD model based on the Karhunen-Loève transformation technique is able to use only part of the POD modes to obtain a high accuracy approximation. The snapshot reconstruction based on the truncated approximation formula needs to be done depending on additional parameters used in the snapshot generation. Hence, an arbitrary snapshot can be defined as follows:

$$\boldsymbol{u}^j = \sum_{k=1}^{K} \bar{\Phi}^k \cdot a_k^j \qquad (2)$$

where $\mathbf{u}^j$ is the vector of the arbitrary snapshot, $\bar{\Phi}^k$ is the *k*-element of the truncated orthogonal basis and a_k^j is the unknown coefficient vector related to the parameters used to create the snapshots. The foregoing approximation is valid only for snapshots used to build the POD basis. In proposed HROM, the radial basis interpolation functions were applied as the RBF interpolation is mostly used for multidimensional approximation. The matrix of coefficients **V** is postulated to be combination of Radial Basis Functions (RBF)

$$\boldsymbol{V} = \mathbf{B} \cdot \mathbf{G} \qquad (3)$$

where matrix G is interpolation functions matrix, filled by interpolation functions (Ostrowski et al., 2005). In this study, the thin plate spline radial function with the smoothing factor was employed:

$$f_i\left(\left|k - k^i\right|\right) = \left(\frac{\left|k-k^i\right|}{r}\right)^2 \cdot ln\left(\frac{\left|k-k^i\right|}{r}\right) \qquad (4)$$

where $\left|k - k^i\right|$ is the distance between the current set of the parameters k and the reference set of the parameters k^i (here taken as parameters used to generate snapshots), *r* is the smoothing factor. Finally, the snapshot generation by use of the arbitrary parameter set *k* can be defined by the following equation:

$$\boldsymbol{u}^a(k) = \bar{\mathbf{\Phi}} \cdot \mathbf{B} \cdot \mathbf{f}^a(k) \quad (5)$$

where $\boldsymbol{u}^a(k)$ is the calculated snapshot based on the arbitrary parameter set k and $\mathbf{f}^a(k)$ stands for column vector of interpolation functions defined in Eq. (4), **B** is the matrix of the unknown coefficients of selected combination. The implementation of RBF into the POD model reduces the dimensionality of ROM to the number of unknown parameters *k*. The unknown parameters are defined as the boundary conditions of the CO_2 two-phase ejector as follows:

- Motive nozzle pressure
- Motive nozzle specific enthalpy
- Suction nozzle pressure
- Suction nozzle specific enthalpy

- Outlet pressure

The specific enthalpy for the motive nozzle and the suction nozzle was defined to perform the calculations either in the one-phase conditions or in the two-phase conditions. The snapshot generated from the CFD results was prepared similar to the snapshot based on the experimental data to use both inputs in the HROM basis. The single snapshot was defined as a set of the motive nozzle and the suction nozzle MFRs for one set of boundary condition.

3.2 CFD model

The CFD model of the R744 two-phase ejector was developed by Smolka et al. (2013). The enthalpy-based energy equation formulation was implemented to obtain real fluid properties of CO_2 flow in the two-phase region. The fluid properties of the R744 two-phase flow were given from REFPROP libraries (Lemmon et al., 2013). The CFD model calculations were performed based on two fluid flow assumption models: homogeneous equilibrium model (HEM) and modified homogeneous relaxation model (HRM). HEM was used to predict MFRs in the supercritical region and close to the critical point for which HEM application range was defined (Palacz et al., 2015). The modified HRM let to obtain the motive nozzle and the suction nozzle MFR accuracy within ±10% for subcritical operating regime due to the optimisation of the relaxation time correlation (Haida et al., 2018b). The CFD model with both fluid flow assumptions was validated as well as the investigation of the numerical mesh grid was performed (Palacz et al., 2016). Moreover, the automation of the geometry and mesh preparation together with the CFD calculation and the post-processing was done by developing of the *ejectorPL* platform. The foregoing platform was successfully used in several numerical investigations of the CO_2 ejector (Bodys et al., 2017; Haida et al., 2016). Therefore, the CFD results used to generate the HROM basis were given by use of the *ejectorPL* platform.

3.3 Experimental data

The test campaign was carried out on the R744 multi-ejector vapour compression test rig in the SINTEF laboratory in Trondheim, Norway. The multi-ejector module was utilised either in a single operation for each vapour ejector or in parallel operation. The test facility is fully equipped with pressure, temperature and the mass flow rate sensors for which the accuracies were taken from the product data-sheet. The temperature was measured by the resistance thermometers PT1000 with the accuracy of ±0.3 + 0.005t, where t is the temperature in °C. The piezoelectric transmitter was used to measure the pressure with the accuracy of ±0.3% of reading. The mass flow rate measurement was done by use of the Coriolis type RHM06 and RHM15 transducers and the accuracy was of ±0.2% of reading. The output signals from sensors installed in the test rig were processed and transmitted by the Danfoss control unit to the Danfoss Minilog system.

3.4 HROM validation

A use of the experimental data together with the high-accurate CFD results to generate HROM of each CO_2 ejector let to evaluate the ejector performance at the refrigeration, air-conditioning and heat-pump operating conditions in the supermarket system. The ejector work can be presented by the use of the mass entrainment ratio and ejector efficiency definitions. The mass entrainment ratio is the ratio between the suction nozzle MFR and the motive nozzle MFR:

$$\chi = \frac{\dot{m}_{SN}}{\dot{m}_{MN}} \qquad (9)$$

where χ is the mass entrainment ratio and $\dot{m}$ is the mass flow rate of the motive nozzle (MN) and the suction nozzle (SN). In this paper, the mass entrainment ratio was presented for each investigated ejector to indicate the area of best ejector performance at different operating conditions. Hence, HROMs of the ejectors installed in the multi-ejector module were validated with the experimental data to ensure the high accuracy of the MFRs prediction. The MFR discrepancy of HROM was calculated as the relative error between the experimental data and the model result:

$$\delta = 1 - \frac{\dot{m}_{HROM}}{\dot{m}_{exp}} \qquad (10)$$

where δ is the relative error of the motive nozzle MFR or the suction nozzle MFR obtained by HROM.

Table 2 presents the set of the HROMs validation procedure results as the MFR discrepancy range of each HROM for all the considered experimental points. The validation procedure of four ejectors was presented for HROM based on the CFD results together with 50% or 100% of the available experimental data. The HROMs based on the CFD results together with 50% of all experimental data obtained the motive nozzle MFR discrepancy within ±5% for each ejector. The suction nozzle MFR discrepancy was within ±10% for VEJ1 and VEJ2 and ±15% for VEJ3 and VEJ4. It can be seen that the use of 100% of the experimental data to build HROM basis improved the motive nozzle and suction nozzle MFR accuracy of the HROMs within ±1%.. The HROM of the vapour ejectors installed in the multi-ejector module indicated satisfactory accuracy within the specified operational envelope. Hence, the performance mapping of each investigated ejector was done for different application operating conditions existed in the R744 supermarket HVAC&R system.

Table 2. The set of the HROM motive nozzle and suction nozzle MFR accuracies for all experimental points considered in the validation.

Input data	VEJ1		VEJ2		VEJ3		VEJ4	
	$\lvert\delta_{MN}\rvert$	$\lvert\delta_{SN}\rvert$	$\lvert\delta_{MN}\rvert$	$\lvert\delta_{SN}\rvert$	$\lvert\delta_{MN}\rvert$	$\lvert\delta_{SN}\rvert$	$\lvert\delta_{MN}\rvert$	$\lvert\delta_{SN}\rvert$
CFD + 50% experimental data	< 5%	< 10%	< 5%	< 10%	< 5%	< 15%	< 5%	< 15%
CFD + 100% experimental data	< 1%	< 1%	< 1%	< 1%	< 1%	< 1%	< 1%	< 1%

4. R744 MULTI-EJECTOR REFRIGERATION SYSTEM ENERGY PERFORMANCE

The entrainment possibilities of the ejectors installed in the multi-ejector module at different ambient conditions and pressure lifts let to evaluate the performance of the R744 multi-ejector module and indicate the proper pressure lift at specified ambient temperature. Therefore, Figure 3 presents the motive nozzle operating conditions selected to the performance mapping of each ejector. The operating points were defined for the ambient temperature in the range from 15 °C to 40 °C based on the operating conditions presented in the work of Gullo et al. (2017) to obtain best performance of the gas cooler in the R744 HVAC&R supermarket system. The motive nozzle pressure was defined in the range from 50 bar to approximately 110 bar. Therefore, the operating conditions were within the HROM operating regime and the performance mapping of four investigated ejectors was done.

Figure 4 presents the mass entrainment ratio map of the ejectors installed in the R744 multi-ejector module. The motive nozzle conditions were set for different ambient temperature in the range from 15 °C to 40 °C according to the operating conditions presented in Figure 3. The suction nozzle pressure was of 26 bar with the defined superheat of 8 °C typical for R744 supermarket refrigeration system. The pressure lift was in the range from 1 bar to 15 bar. The green area presents the best entrainment ratio of each ejector above 0.3, whereas yellow area indicates entrainment ratio below 0.3 and the non-suction flow is shown in a red area. It can be seen that each ejector obtained highest mass entrainment ratio for pressure lift of 1 bar for each defined ambient temperature. Although, the high value of the mass entrainment ratio above 0.3 was obtained for pressure lift below 6 bar for VEJ1 and below 10 bar for VEJ2, VEJ3 and VEJ4, respectively. The mass entrainment ratio rapidly dropped for pressure lift above 8 bar and the ambient temperature below 30 °C for pressure lift above 8 bar and the ambient temperature above 30 °C. Therefore, the multi-ejector module was able to obtain the best performance and improve the system energy performance at specified pressure lift ranges either in single ejector working mode or in parallel working mode.

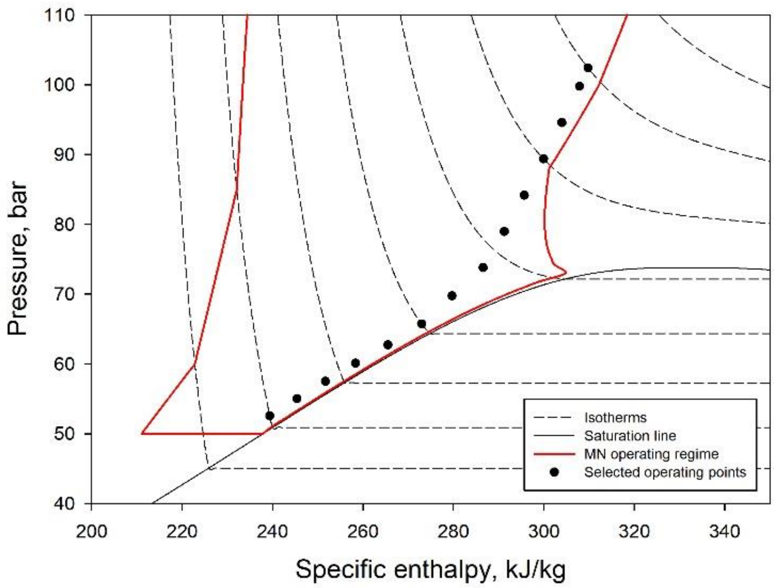

Figure 3. The R744 pressure-specific enthalpy diagram of selected motive nozzle operating points.

(a)

Δp, bar															
15.0	0.00	0.00	0.00	0.00	0.00	0.00	0.00	0.00	0.00	0.00	0.00	0.06	0.15	0.17	
14.0	0.00	0.00	0.00	0.00	0.00	0.00	0.00	0.00	0.00	0.00	0.00	0.07	0.15	0.17	
13.0	0.00	0.00	0.00	0.00	0.00	0.00	0.00	0.00	0.00	0.00	0.02	0.09	0.15	0.17	
12.0	0.00	0.00	0.00	0.00	0.00	0.00	0.00	0.01	0.02	0.03	0.05	0.11	0.15	0.16	
11.0	0.00	0.00	0.00	0.00	0.00	0.00	0.01	0.03	0.05	0.06	0.09	0.13	0.15	0.16	
10.0	0.00	0.00	0.00	0.00	0.00	0.00	0.03	0.06	0.07	0.10	0.13	0.15	0.15	0.15	
9.0	0.00	0.00	0.02	0.03	0.04	0.04	0.07	0.08	0.10	0.13	0.16	0.17	0.15	0.14	
8.0	0.02	0.04	0.06	0.08	0.09	0.09	0.11	0.11	0.13	0.16	0.19	0.19	0.15	0.14	
7.0	0.06	0.08	0.12	0.14	0.15	0.15	0.15	0.15	0.16	0.19	0.22	0.20	0.15	0.13	
6.0	0.10	0.14	0.18	0.21	0.22	0.23	0.21	0.19	0.19	0.22	0.24	0.21	0.15	0.13	
5.0	0.15	0.20	0.25	0.28	0.30	0.30	0.26	0.23	0.22	0.25	0.26	0.22	0.16	0.14	
4.0	0.20	0.25	0.31	0.35	0.37	0.37	0.32	0.27	0.26	0.27	0.28	0.24	0.17	0.14	
3.0	0.26	0.31	0.37	0.41	0.44	0.44	0.37	0.32	0.29	0.30	0.30	0.25	0.18	0.15	
2.0	0.31	0.37	0.43	0.48	0.51	0.50	0.43	0.37	0.33	0.33	0.32	0.26	0.19	0.16	
1.0	0.36	0.42	0.48	0.53	0.56	0.55	0.48	0.41	0.37	0.35	0.33	0.27	0.20	0.17	
	15.0	17.0	19.0	21.0	23.0	25.0	27.0	29.0	31.0	33.0	35.0	37.0	39.0	40.0	t_{MN}, °C
	52.6	55.0	57.5	60.1	62.7	65.7	69.7	73.8	79.0	84.2	89.4	94.6	99.8	102.4	p_{MN}, bar

(b)

Δp, bar															
15.0	0.00	0.00	0.00	0.00	0.00	0.00	0.00	0.00	0.00	0.00	0.00	0.00	0.02	0.04	
14.0	0.00	0.00	0.00	0.00	0.00	0.00	0.00	0.00	0.00	0.01	0.02	0.05	0.08	0.09	
13.0	0.00	0.00	0.00	0.00	0.00	0.00	0.00	0.01	0.04	0.06	0.08	0.11	0.14	0.15	
12.0	0.00	0.00	0.00	0.00	0.00	0.00	0.00	0.04	0.08	0.12	0.15	0.18	0.20	0.20	
11.0	0.00	0.00	0.00	0.00	0.00	0.00	0.01	0.07	0.13	0.17	0.21	0.24	0.25	0.25	
10.0	0.00	0.00	0.00	0.00	0.00	0.00	0.05	0.12	0.18	0.23	0.26	0.29	0.29	0.28	
9.0	0.00	0.00	0.00	0.01	0.02	0.04	0.10	0.17	0.23	0.27	0.31	0.32	0.31	0.30	
8.0	0.00	0.00	0.03	0.06	0.08	0.11	0.17	0.24	0.28	0.32	0.34	0.34	0.31	0.30	
7.0	0.01	0.04	0.08	0.12	0.15	0.19	0.25	0.30	0.34	0.36	0.36	0.34	0.30	0.29	
6.0	0.05	0.09	0.14	0.19	0.23	0.28	0.33	0.37	0.39	0.40	0.38	0.34	0.29	0.27	
5.0	0.09	0.15	0.20	0.26	0.32	0.37	0.41	0.44	0.45	0.44	0.40	0.33	0.27	0.25	
4.0	0.14	0.20	0.27	0.33	0.40	0.45	0.48	0.50	0.50	0.47	0.42	0.33	0.26	0.24	
3.0	0.18	0.25	0.33	0.40	0.47	0.53	0.56	0.57	0.54	0.50	0.43	0.34	0.26	0.24	
2.0	0.23	0.31	0.39	0.47	0.54	0.60	0.62	0.62	0.59	0.53	0.44	0.35	0.27	0.25	
1.0	0.27	0.36	0.44	0.53	0.61	0.66	0.68	0.67	0.62	0.56	0.46	0.36	0.29	0.26	
	15.0	17.0	19.0	21.0	23.0	25.0	27.0	29.0	31.0	33.0	35.0	37.0	39.0	40.0	t_{MN}, °C
	52.6	55.0	57.5	60.1	62.7	65.7	69.7	73.8	79.0	84.2	89.4	94.6	99.8	102.4	p_{MN}, bar

(c)

Δp, bar															
15.0	0.00	0.00	0.00	0.00	0.00	0.00	0.00	0.00	0.00	0.00	0.00	0.00	0.02	0.03	
14.0	0.00	0.00	0.00	0.00	0.00	0.00	0.00	0.00	0.00	0.01	0.02	0.04	0.07	0.08	
13.0	0.00	0.00	0.00	0.00	0.00	0.00	0.00	0.01	0.05	0.07	0.08	0.10	0.12	0.13	
12.0	0.00	0.00	0.00	0.00	0.00	0.00	0.00	0.03	0.10	0.13	0.15	0.16	0.17	0.18	
11.0	0.00	0.00	0.00	0.00	0.00	0.00	0.00	0.07	0.15	0.20	0.22	0.22	0.22	0.22	
10.0	0.01	0.01	0.00	0.00	0.00	0.00	0.02	0.12	0.22	0.27	0.28	0.28	0.27	0.27	
9.0	0.04	0.04	0.03	0.02	0.01	0.00	0.08	0.19	0.28	0.33	0.34	0.33	0.32	0.31	
8.0	0.08	0.10	0.09	0.09	0.09	0.09	0.17	0.27	0.35	0.39	0.39	0.37	0.35	0.34	
7.0	0.14	0.18	0.17	0.17	0.18	0.19	0.27	0.35	0.41	0.43	0.43	0.40	0.38	0.37	
6.0	0.21	0.26	0.26	0.26	0.28	0.31	0.37	0.43	0.46	0.47	0.45	0.42	0.40	0.39	
5.0	0.27	0.35	0.36	0.36	0.37	0.41	0.46	0.50	0.50	0.49	0.46	0.43	0.41	0.41	
4.0	0.32	0.43	0.44	0.44	0.46	0.51	0.54	0.55	0.53	0.50	0.47	0.44	0.42	0.41	
3.0	0.36	0.48	0.51	0.51	0.53	0.58	0.59	0.59	0.55	0.51	0.47	0.44	0.42	0.41	
2.0	0.37	0.50	0.55	0.57	0.59	0.63	0.63	0.61	0.56	0.51	0.46	0.44	0.42	0.41	
1.0	0.37	0.51	0.57	0.60	0.63	0.66	0.66	0.63	0.56	0.51	0.46	0.43	0.41	0.40	
	15.0	17.0	19.0	21.0	23.0	25.0	27.0	29.0	31.0	33.0	35.0	37.0	39.0	40.0	t_{MN}, °C
	52.6	55.0	57.5	60.1	62.7	65.7	69.7	73.8	79.0	84.2	89.4	94.6	99.8	102.4	p_{MN}, bar

(d)

Δp, bar															
15.0	0.00	0.00	0.00	0.00	0.00	0.00	0.00	0.00	0.00	0.00	0.00	0.00	0.03	0.06	
14.0	0.01	0.00	0.00	0.00	0.00	0.00	0.00	0.00	0.00	0.02	0.05	0.05	0.08	0.10	
13.0	0.01	0.00	0.00	0.00	0.00	0.00	0.00	0.00	0.04	0.08	0.12	0.12	0.13	0.14	
12.0	0.00	0.00	0.00	0.00	0.00	0.00	0.00	0.04	0.09	0.15	0.19	0.20	0.18	0.19	
11.0	0.00	0.00	0.00	0.00	0.00	0.00	0.03	0.10	0.15	0.22	0.27	0.28	0.25	0.23	
10.0	0.01	0.00	0.00	0.00	0.00	0.02	0.09	0.16	0.22	0.29	0.35	0.35	0.31	0.28	
9.0	0.02	0.03	0.03	0.04	0.04	0.08	0.16	0.24	0.30	0.36	0.41	0.42	0.36	0.32	
8.0	0.04	0.06	0.08	0.09	0.11	0.15	0.24	0.32	0.37	0.43	0.47	0.46	0.39	0.33	
7.0	0.07	0.11	0.15	0.17	0.18	0.24	0.32	0.39	0.43	0.47	0.50	0.47	0.37	0.32	
6.0	0.10	0.16	0.21	0.25	0.28	0.34	0.41	0.45	0.48	0.50	0.51	0.45	0.35	0.31	
5.0	0.13	0.21	0.28	0.33	0.38	0.45	0.48	0.51	0.51	0.52	0.51	0.43	0.33	0.29	
4.0	0.17	0.25	0.34	0.41	0.47	0.53	0.54	0.55	0.54	0.53	0.50	0.41	0.31	0.28	
3.0	0.20	0.29	0.40	0.48	0.55	0.60	0.59	0.58	0.56	0.54	0.49	0.40	0.30	0.27	
2.0	0.24	0.34	0.44	0.53	0.60	0.64	0.62	0.60	0.57	0.54	0.48	0.39	0.30	0.27	
1.0	0.27	0.37	0.48	0.58	0.65	0.67	0.64	0.62	0.58	0.54	0.48	0.39	0.30	0.28	
	15.0	17.0	19.0	21.0	23.0	25.0	27.0	29.0	31.0	33.0	35.0	37.0	39.0	40.0	t_{MN}, °C
	52.6	55.0	57.5	60.1	62.7	65.7	69.7	73.8	79.0	84.2	89.4	94.6	99.8	102.4	p_{MN}, bar

Figure 4. The mass entrainment ratio map of four ejectors installed in the R744 multi-ejector module: (a) VEJ1; (b) VEJ2; (c) VEJ3; (d) VEJ4.

5. CONCLUSIONS

The performance mapping of the four CO_2 fixed ejectors installed in the multi-ejector module was done. The results were performed for a wide range of the operating conditions to cover the utilisation performance of the ejectors in the R744 HVAC&R supermarket system. The investigation was done based on the HROM of each investigated ejector. The HROM was generated by use of the CFD results and the experimental data. Moreover, the operational envelope of the HROMs was defined to cover the wide operating regime in the CO_2 supermarket system at various ambient temperature. The validation procedure of the HROMs confirmed that the reduced model of each ejector predicted the motive nozzle and the suction nozzle MFR with satisfactory accuracy. Moreover, the HROM was successfully implemented to the Modelica dynamic simulations of the R744 refrigeration supermarket system as the result of the fast HROM computations when compared to the CFD model computational time.

The mass entrainment ratio map of all four ejectors indicated the best performance area of each ejector at different ambient temperature in the range from 15 °C to 40 °C. Moreover, the limitation of the pressure was indicated for each ejector. The high value of the pressure lift together with the high efficiency of each ejector let to utilise the multi ejector equipped with the investigated ejectors at similar efficiency either in single operating mode or in parallel mode. Hence, the investigation of the multi-ejector performance based on the proposed HROMs of the ejectors should be done to analyse the energy performance improvement of the R744 multi-ejector HVAC&R system for supermarket application.

ACKNOWLEDGEMENTS

The authors gratefully acknowledge the financial support of the Research Council of Norway through project No. 244009/E20.

NOMENCLATURE

h	specific enthalpy (J/kg)	s	specific entropy ($J \cdot kg^{-1} \cdot K^{-1}$)
$\dot{m}$	mass flow rate (kg/s)	t	temperature (°C)
p	pressure (bar)	Δp	pressure lift (bar)

REFERENCES

Banasiak, K., Hafner, A., Kriezi, E.E., Madsen, K.B., Birkelund, M., Fredslund, K., Olsson, R., 2015. Development and performance mapping of a multi-ejector expansion work recovery pack for R744 vapour compression units. Int. J. Refrigeration 57, 265-276.

Besagni, G., Mereu, R., Inzoli, F., 2016. Ejector refrigeration: A comprehensive review. Renew. Sustain. Energy Rev. 53, 373-407.

Bodys, J., Palacz, M., Haida, M., Smolka, J., Nowak, A.J., Banasiak, K., Hafner, A., 2017. Full-scale multi-ejector module for a carbon dioxide supermarket refrigeration system: Numerical study of performance evaluation. Energy Convers. Manag. 138, 312-326.

Cecchinato, L., Corradi, M., Minetto, S., 2010. Energy performance of supermarket refrigeration and air conditioning integrated systems. Appl. Therm. Eng. 30, 1946-1958.

Elbel, S., Hrnjak, P., 2004. Flash gas bypass for improving the performance of transcritical R744 systems that use microchannel evaporators. Int. J. Refrigeration 27, 724-735.

Gullo, P., Hafner, A., Cortella, G., 2017. Multi-ejector R744 booster refrigerating plant and air conditioning system integration – A theoretical evaluation of energy benefits for supermarket applications. Int. J. Refrigeration 75, 164-176.

Hafner, A., Forsterling, S., Banasiak, K., 2014. Multi-ejector concept for R-744 supermarket refrigeration. Int. J. Refrigeration 43, 1-13.

Haida, M., Smolka, J., Hafner, A., Ostrowski, Z., Palacz, M., Nowak, A.J., Banasiak, K., 2018a. System model derivation of the CO2 two-phase ejector based on the CFD-based reduced-order model. Energy.

Haida, M., Smolka, J., Hafner, A., Palacz, M., Banasiak, K., Nowak, A.J., 2018b. Modified homogeneous relaxation model for the R744 trans-critical flow in a two-phase ejector. Int. J. Refrigeration 85, 314-333.

Haida, M., Smolka, J., Palacz, M., Bodys, J., Nowak, A.J., Bulinski, Z., Fic, A., Banasiak, K., Hafner, A., 2016. Numerical investigation of an R744 liquid ejector for supermarket refrigeration systems. Thermal Science 20, 1259-1269.

Kim, M.H., Pettersen, J., Bullard, C.W., 2004. Fundamental process and system design issues in CO2 vapor compression systems. Prog. Energy Combust. Sci. 30, 119-174.

Kornhauser, A.A., 1990. The Use of an Ejector as a Refrigerant Expander, International Refrigeration and Air Conditioning Conference. Purdue e-Pubs, Purdue University, p. 11.

Lemmon, E.W., Huber, M.l., McLinden, M.O., 2013. NIST Standard Reference Database 23: Reference Fluid Thermodynamic and Transport Properties-REFPROP, Standard Reference Data Program, 9.1 ed. National Institute of Standards and Technology, Gaithersburg.

Ostrowski, Z., Białecki, R.A., Kassab, A.J., 2005. Estimation of constant thermal conductivity by use of Proper Orthogonal Decomposition. Computational Mechanics 37, 52-59.

Ostrowski, Z., Białecki, R.A., Kassab, A.J., 2008. Solving inverse heat conduction problems using trained POD-RBF network inverse method. Inverse Problems in Science and Engineering 16, 39-54.

Palacz, M., Smolka, J., Fic, A., Bulinski, Z., Nowak, A.J., Banasiak, K., Hafner, A., 2015. Application range of the HEM approach for CO2 expansion inside two-phase ejectors for supermarket refrigeration systems. Int. J. Refrigeration.

Palacz, M., Smolka, J., Kus, W., Fic, A., Bulinski, Z., Nowak, A.J., Banasiak, K., Hafner, A., 2016. CFD-based shape optimisation of a CO2 two-phase ejector mixing section. Appl. Therm. Eng. 95, 62-69.

Sharma, V., Fricke, B., Bansal, P., 2014. Comparative analysis of various CO2 configurations in supermarket refrigeration systems. Int J Refrig. Int. Du Froid 46, 86-99.

Smolka, J., Bulinski, Z., Fic, A., Nowak, A.J., Banasiak, K., Hafner, A., 2013. A computational model of a transcritical R744 ejector based on a homogeneous real fluid approach. Applied Mathematical Modelling 37, 1208-1224.

United Nations Environment, P., Ozone, S., 1987. Handbook for the Montreal Protocol on Substances that Deplete the Ozone Layer.